BALANCE OF HELM OF SAILING YACHTS

—— A Shiphydrodynamics Approach on the Problem ——

by

K. NOMOTO AND H. TATANO

UNIVERSITY OF OSAKA

DEPARTMENT OF NAVAL ARCHITECTURE

ABSTRACT

Tank tests of three typical sailing hulls are carried out. Colin Archer redningskoite, a medium displacement cruising cutter and an IOR Q-tonner are taken. An emphasis is laid upon lateral resistance and its centre of action, namely CLR.

The experimental results are compared with existing methods of estimating lateral resistance and/or CLR, including the popular method of geometric CLR, slender body lift theory and the method of Gerritsma.

Then we propose a new method; a combination of Gerritsma method and slender body theory. This proved effective for most yacht hull types of the present day.

Finally we deal with a performace prediction based upon the tank test. Sail force data is taken from another experimental source. Balance of helm and its physical mechanism are discussed.

PREFACE

Balance of helm of sailing vessels has long been a popular topic. Sailors have a keen interest in "weather-helm" and "lee-helm" of their ships; naval architects often refer to "Centre of Effort (C.E.)" and "Centre of Lateral Resistance (C.L.R.)" and "Lead". Yet this problem has been dealt with largely on the empirical basis; rather few scientific approach on it.[1] Here we will introduce some experimental and analytical studies on the problem. These studies were performed at the Ship Experiment Tank of Osaka University as a part of a research project on shiphydrodynamics of sailing vessels.

1. TANK TESTS OF THREE TYPICAL YACHT HULLS

1.1 Model Types

We take three typical hull forms: the Colin Archer's "redningskoite" at one end, a light IOR Q-tonner at the other and a medium displacement cruising cutter in between. The lines are shown in Figs.1, 2 and 3 and their principal particulars in Table 1.

Models A and B are fabricated of polyuretane foam plastics with thin outer coat of polyester resin and inboard lining of GRP. Model C is of GRP sandwich construction with PVC-foam core.

Our practice for turbulence stimulation to establish a turbulent boundary layer is two rows of square-section studs put on the hull surface. Arrangement is shown in the lines plans (Figs. 1, 2 and 3). We have a good ship-model correlation with this technique [2].

1.3 Experimental Scheme and Set-up

The tank test was carried out at the Ship Experiment Tank of Osaka University, 100m long, 7.8m wide and 4.6m deep. We measured the resistance, lateral resistance and the centre of lateral resistance at a number of combinations of leeway angle, rudder angle, heel angle and speed.

The set-up is shown in Fig.4. We hold a model hull with a 4-component dynamometer at fixed angles of leeway and heel. Trim and sinkage of the hull are free. The dynamometer is one of the ready-made types supplied by Nisho Electric Instruments Co. Ltd. and it is essentially a multi-column force sensor with bond wire strain-gauge pick-ups.

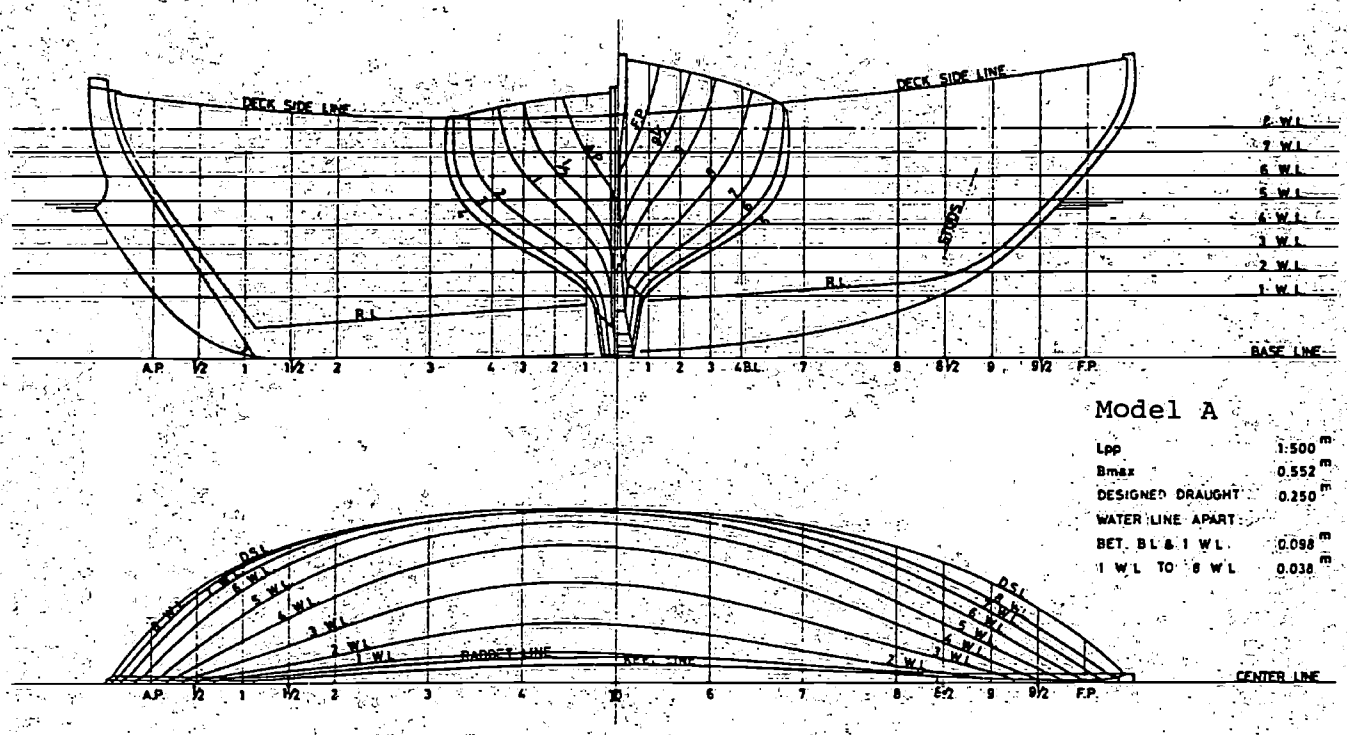

Fig. 1. Lines Plan of Model A

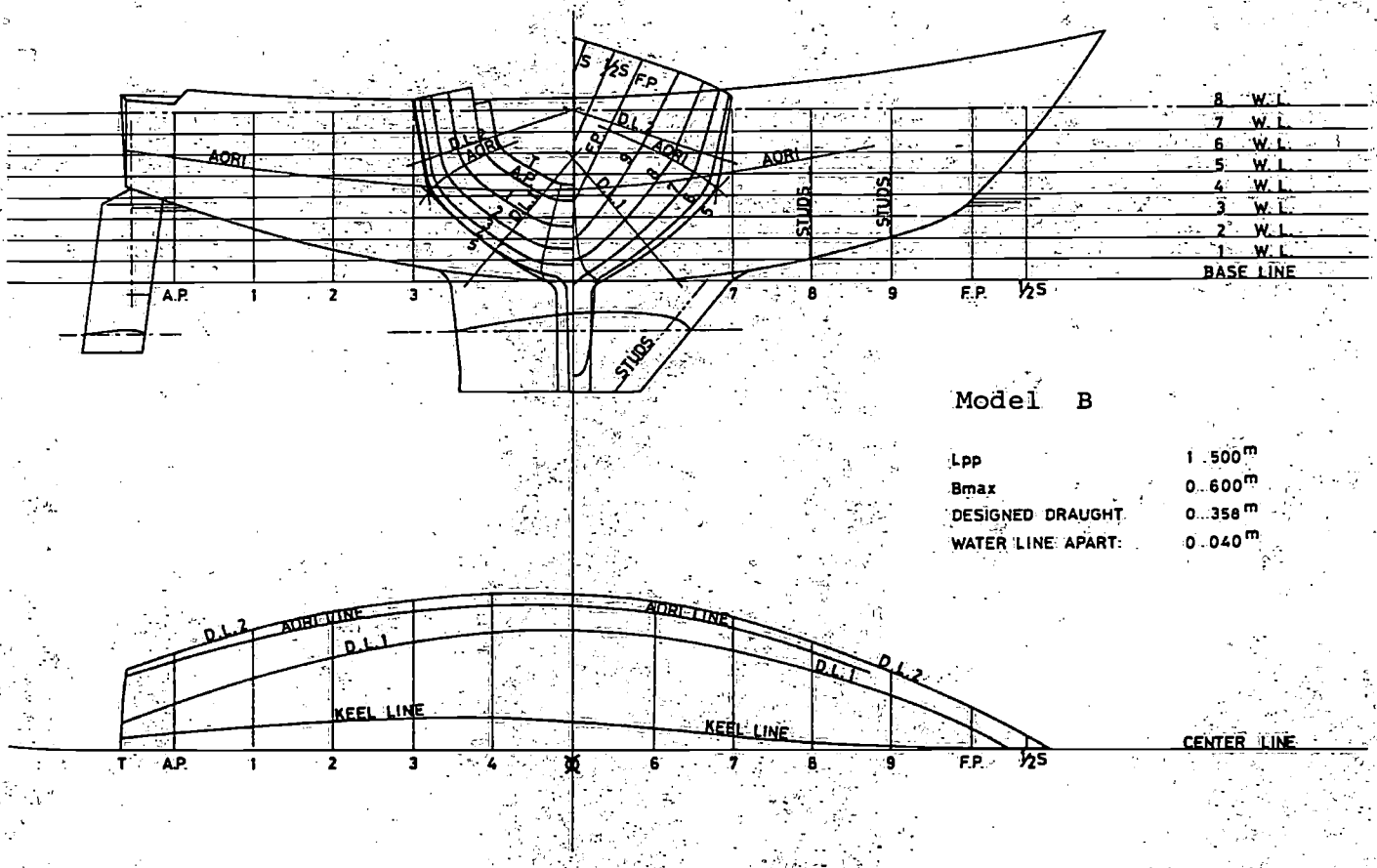

Fig. 2. Lines Plan of Model B

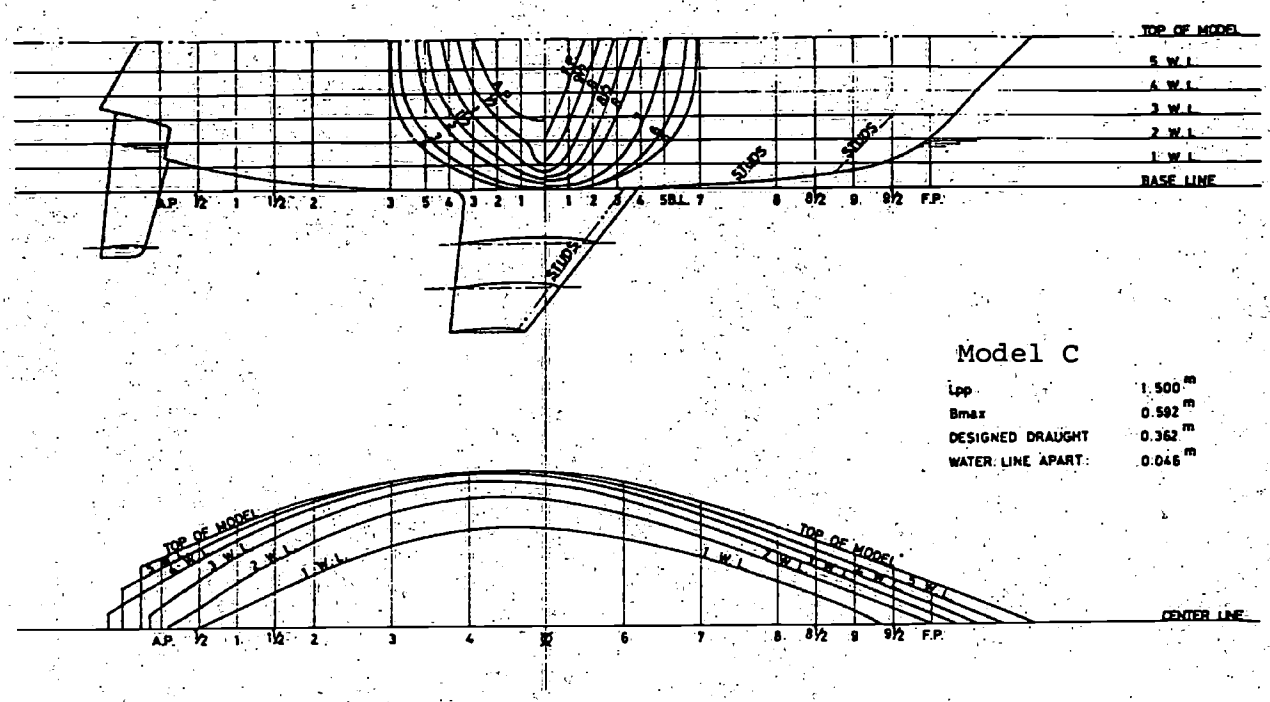

Fig. 3. Lines Plan of Model C

TABLE 1 Principal Particulars of Models

		Redningskoite Model A	Cruising Cutter Model B	Q-Tonner Model C
L_{pp}	(m)	1.500	1.500	1.500
L_{oa}	(m)	1.648	1.846	1.848
L_{wl}	(m)	1.545	1.686	1.594
B_{max}	(m)	0.552	0.600	0.592
B_{wl}	(m)	0.504	0.504	0.489
d_{max}	(m)	0.250	0.358	0.362
d_h (hull)	(m)	0.143	0.150	0.0925
∇ (total,	m^3)	0.04414	0.04344	0.02847
∇_h (hull,	m^3)		0.03898	0.02740
A_h	(m^2)	0.2927	0.1554	0.1133
A_k	(m^2)		0.0905	0.0644
A_R	(m^2)	0.0222	0.0318	0.0213
$A = A_h+A_k+A_R$		0.3149	0.2777	0.1990
$\Delta / (L'/100)^3$		347 *	263 *	204 *
d_h / L_{wl}		0.162 #	0.089	0.058

A_h: main hull lateral area, A_k: fin keel lateral area
A_R: rudder area (including skeg, if any), L' : L_{wl} in feet
* indicates values on sea water, # : d_{max} / L_{wl}.

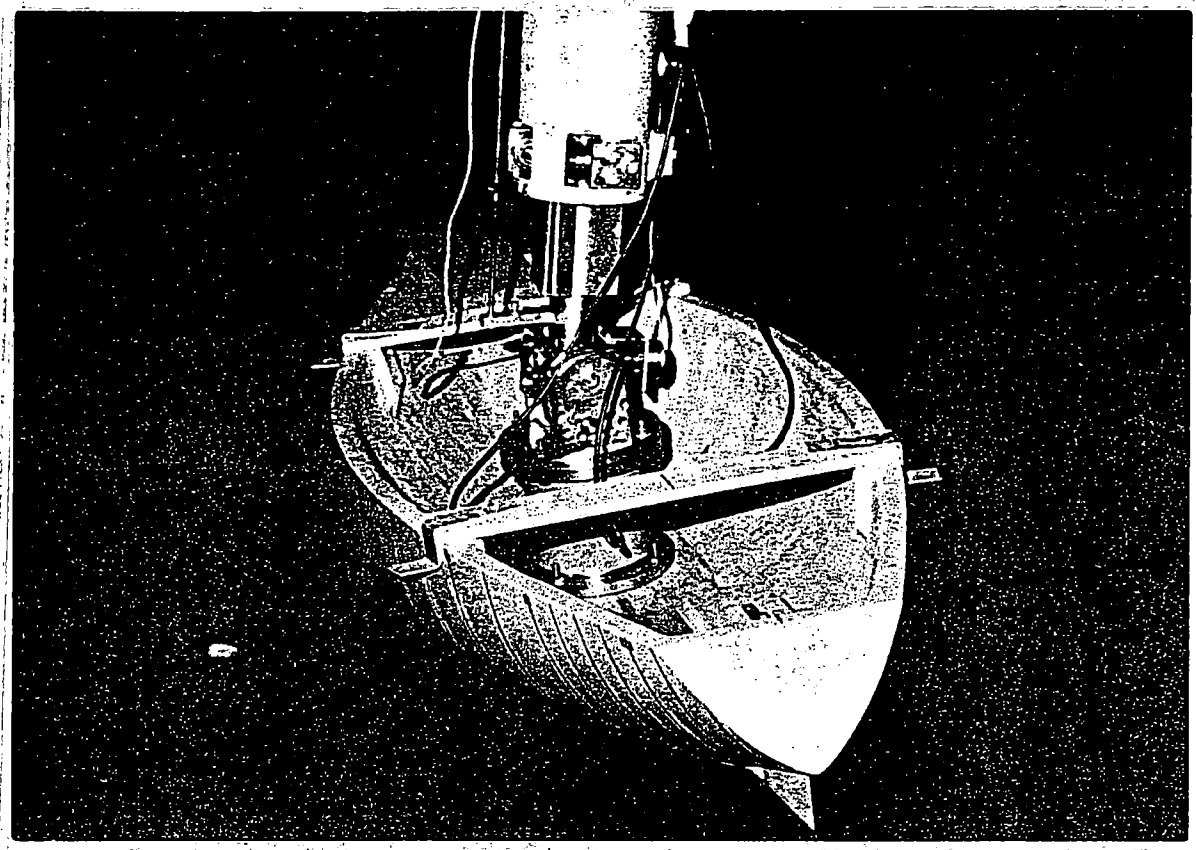

Fig.4. Experimental Set-up

1.3 Experimental Results

Figs.5, 6 and 7 shows the resistance test results without leeway and heel. The total resistance coefficients of different models should not be compared directly however, since the appendage configurations (ballast keel and skeg and rudder) differ immensely among three types. This is interesting but another subject and we will leave it to another occasion.

Figs.9 through 20 illustrate how the lateral resistance and its centre show themselves with different angles of heel and leeway. The effect of rudder deflection to correct a helm balance is also indicated. The figures also show the heeling moment of the lateral resistance. The notations employed are (cf. Fig.8)

β : angle of leeway, positive to port

ϕ : angle of heel, positive to port

δ : rudder angle, positive to starboard rudder

V : ship speed in m/sec.

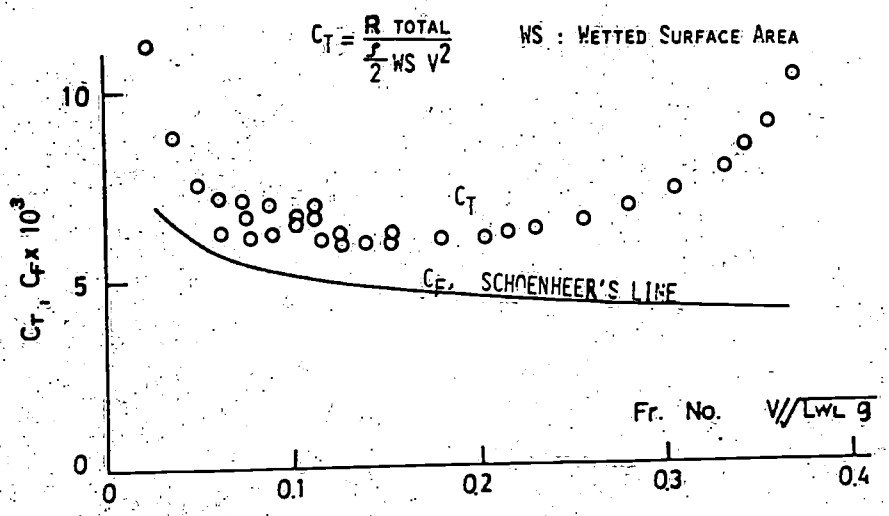

Fig.5 Resistance Test Result of Model A

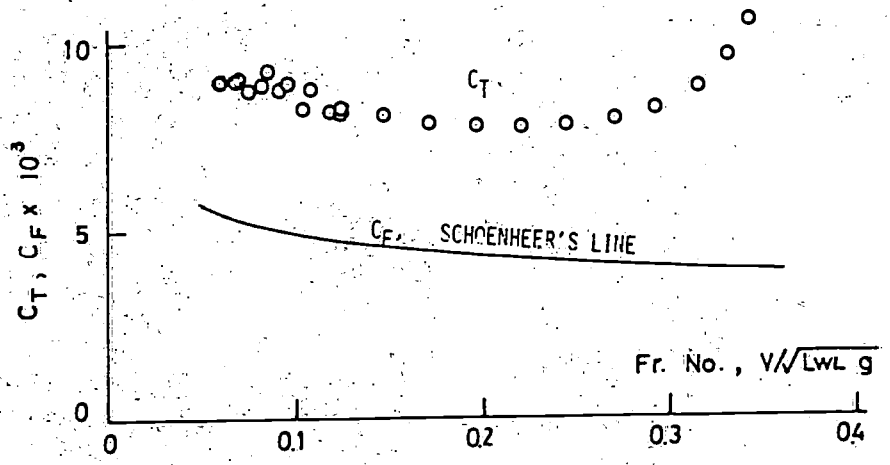

Fig.6 Resistance Test Result of Model B

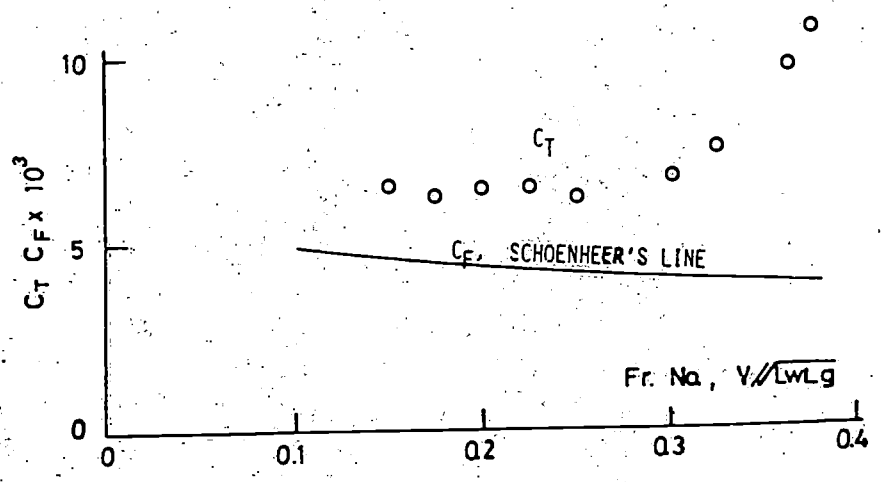

Fig. 7 Resitance Test Result of Model C

ρ : water density in kg $m^{-4} sec^2$

A : lateral projected area of underbody including keel, skeg and rudder

$X' = X / \frac{1}{2}\rho AV^2$, X : longitudinal resistance, negative sign corresponds to aftward force

$Y' = Y / \frac{1}{2}\rho AV^2$, Y : lateral resistance

$N' = N / \frac{1}{2}\rho AL_{wl}V^2$ N : hydrodynamic yaw moment about the midship

$CLR' = \frac{N'}{Y'}$: distance of centre of lateral resistance from the midship in fraction of L_{wl}

$L' = L / \frac{1}{2}\rho AdV^2$, L : heeling moment of lateral resistance about the point "O", that is the middle point of water line on the midship section at upright condition (cf. Fig.8)

d : maximum draught (bottom of keel)

The lateral force Y is normal to the fore-and-aft axis of the yacht, and the resistance X parallel to the axis. The lift and drag of the hull, refering to the wing theory, are then

$$\text{Lift} = Y\cos\beta - X\sin\beta$$
$$\text{Drag} = X\cos\beta + Y\sin\beta \qquad (1)$$

As a remark in interpreting the result, Y is nearly equal to the lift but the drag and X are quite different from each other.

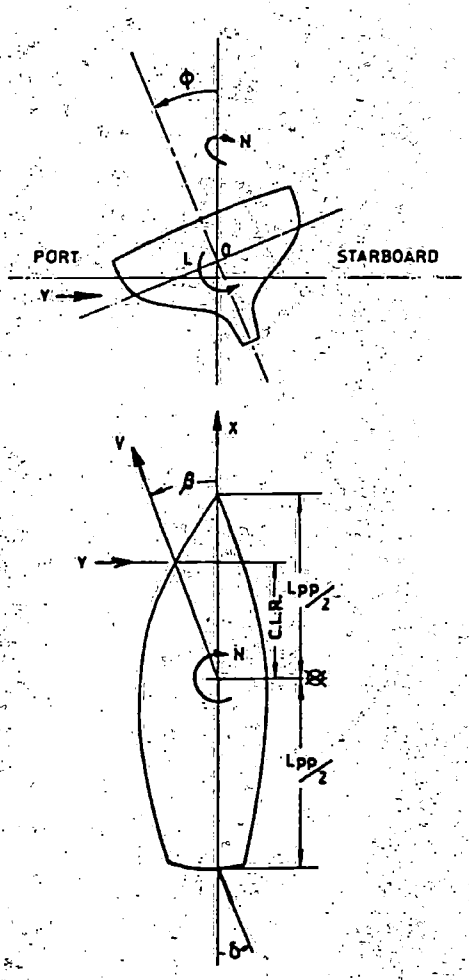

Fig.8 Notations

Findings from the tank tests are:

(1) The lateral resistance of the long-keel model A is considerably smaller than that of the seperate rudder models B and C (Figs. 9,13 and 17). The lift-drag ratio of the hull is accordingly relatively small for A. Windward ability of long-keel boats will not be as good as seperate rudder and fin-keel designs.

(2) The centre of lateral resistance of Model A, with the helm amidship, is at 15 - 20% of L_{wl} forward of midship. For Model B, 5-10% L_{wl} forward, and for Model C it is nearly at the midship. (Figs.9,13 & 17)

(3) The effect of rudder deflection to correct the helm balance is impressive. Only 3° of rudder deflection will move the centre of lateral resistance as much as 10% of L_{wl} for all three models. (Figs. 11, 12,15,16,19 and 20).

(4) The effect of heel on the centre of lateral resistance is rather small. For example, 10° heel shifts the C.L.R. by 6% L_{wl} forward for Model A and 2-3% L_{wl} forward for Models B and C. It can be cancelled by a very slight rudder deflection. (Figs. 11,12,15,16,19 and 20). This suggests that the common trend of weatherhelm in heeled condition can hardly be explained from the hydrodynamic force acting on a heeled hull. We will discuss this point later.

(5) The lateral resistance produces a heeling moment L. We can define the vertical position of the centre of lateral resistance by L/Y. The vertical C.L.R. thus defined is nearly at the bottom of the main hull (canoe body) for all three models. (Figs.9,13 and 17). This can be used in calculating the heeling moment under sail.

2. THEORETICAL ESTIMATION OF LATERAL RESISTANCE AND C.L.R. ---- ----- COMPARISON WITH TANK TEST RESULTS.

We have a number of theories on the lateral force acting upon an obliquely sailing hull. They range from a simple approximation to highly sophisticated computation, but none of them is, in author's view, established one. What we have done here is first to apply a few typical theories to the present three hull forms, Models A, B and C, comparing the results with the tank test data. Next we introduce a new method of estimating the lateral force and moment, based upon a general review on the problem from the hydrodynamics point of view. This is in a sense an improvement of the method of Gerritsma[3] by applying the slender body lift theory to the hull moment. Its result is also compared with the tank test data.

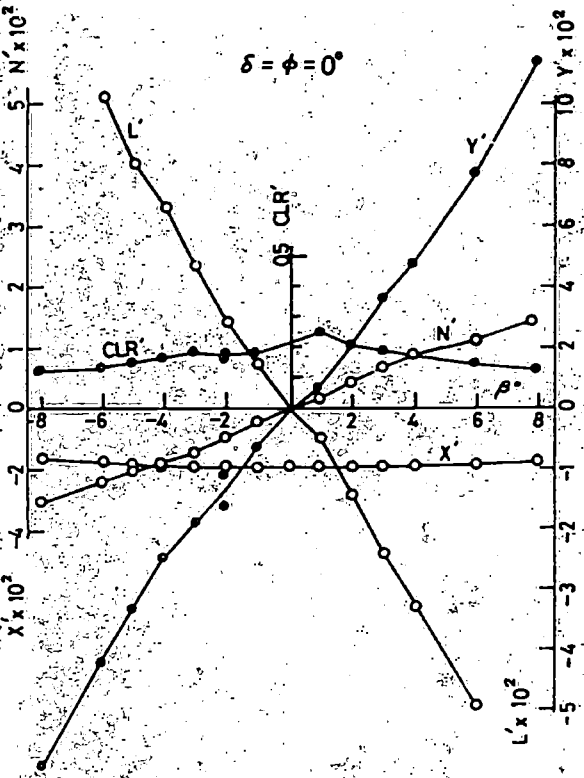

Fig.9 Oblique Tow Test Result of Model A (1)

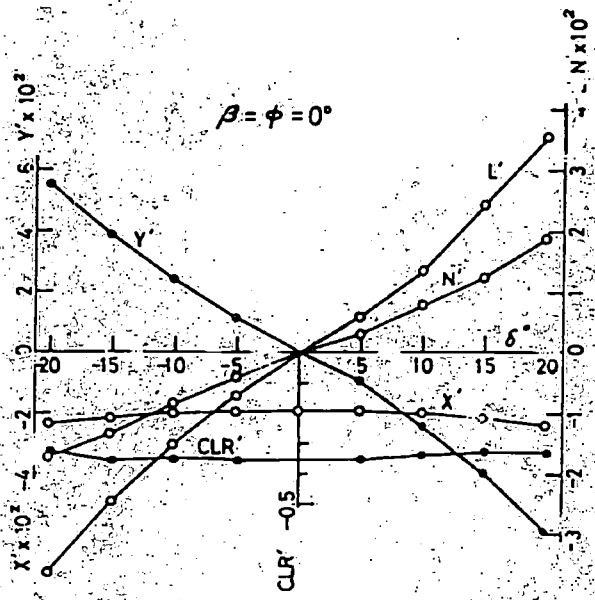

Fig.10 Oblique Tow Test Result of Model A (2)

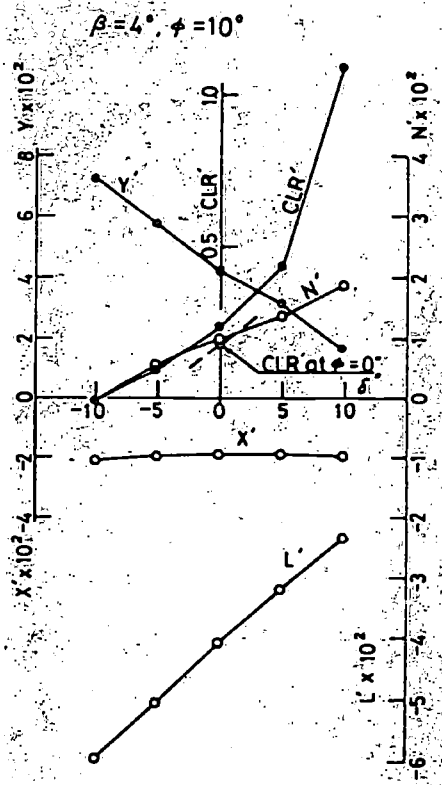

Fig.11 Oblique Tow Test Result of Model A (3)

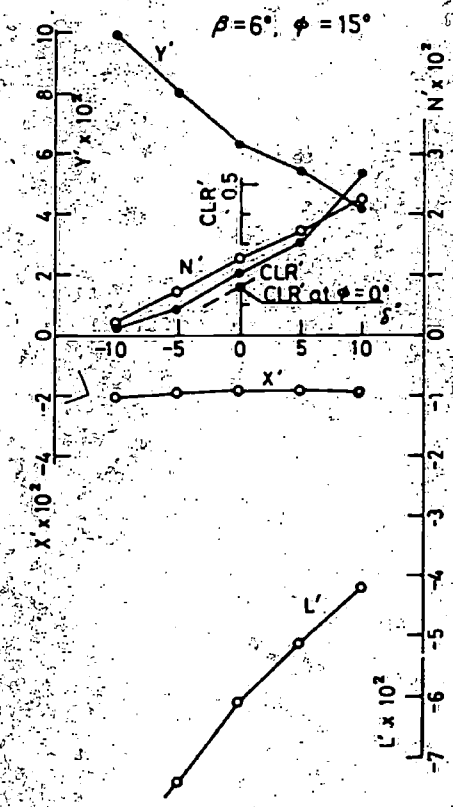

Fig.12 Oblique Tow Test Result of Model A (4)

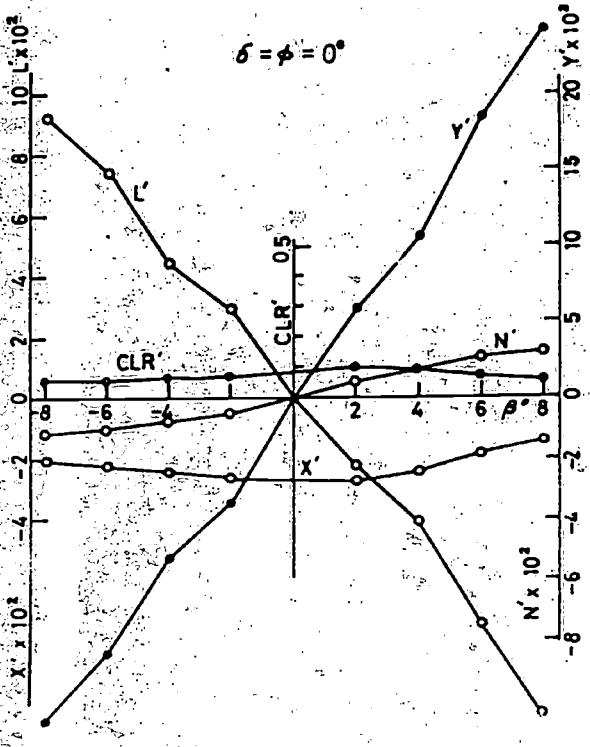

Fig. 13 Oblique Tow Test Result of Model B (1)

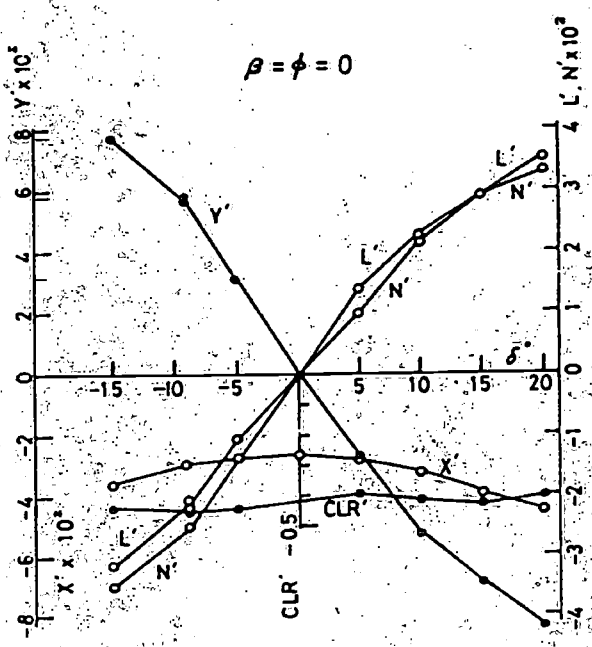

Fig. 14 Oblique Tow Test Result of Model B (2)

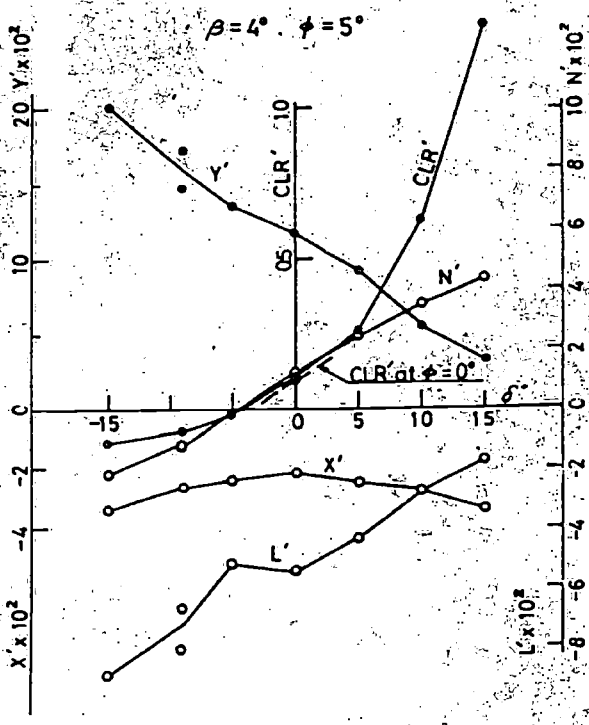

Fig. 15 Oblique Tow Test Result of Model B (3)

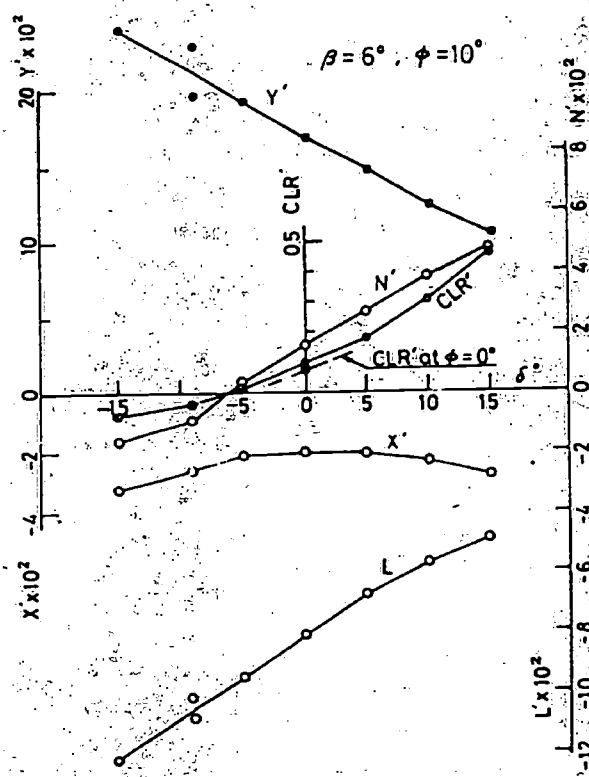

Fig. 16 Oblique Tow Test Result of Model B (4)

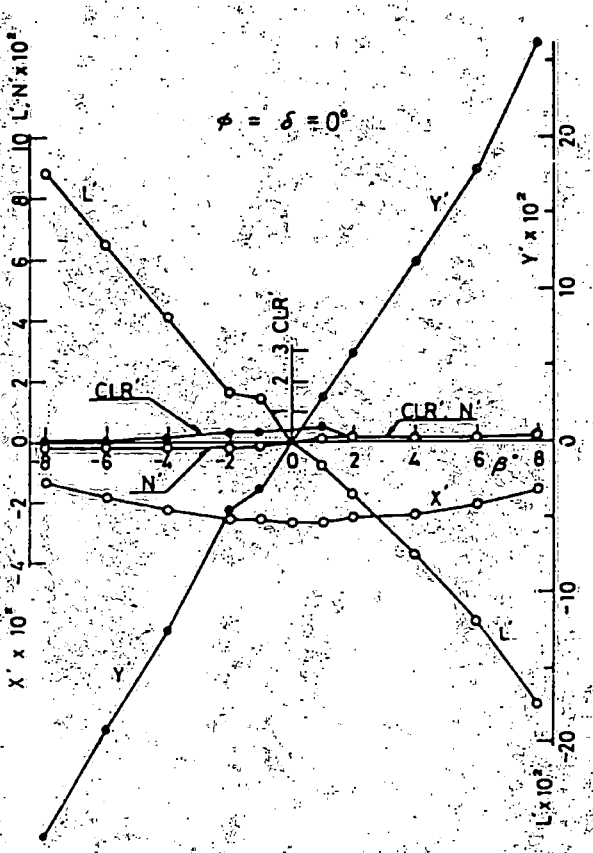

Fig. 17 Oblique Tow Test Result of Model C (1)

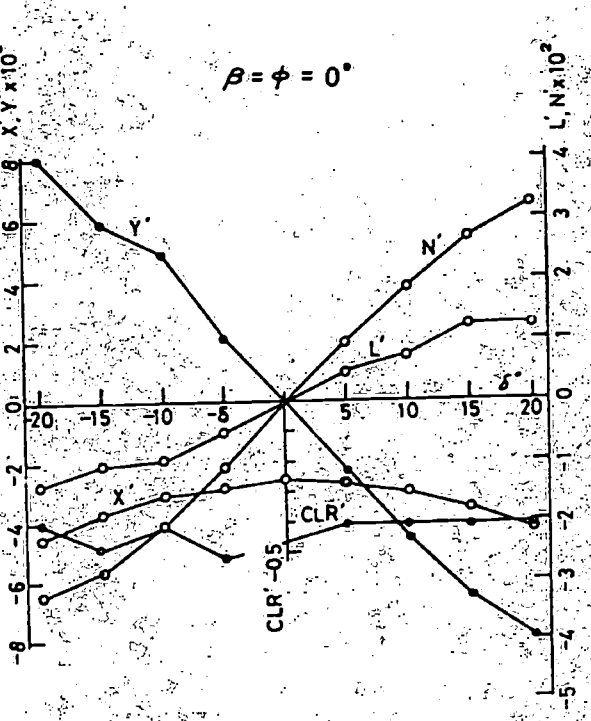

Fig. 18 Oblique Tow Test Result of Model C (2)

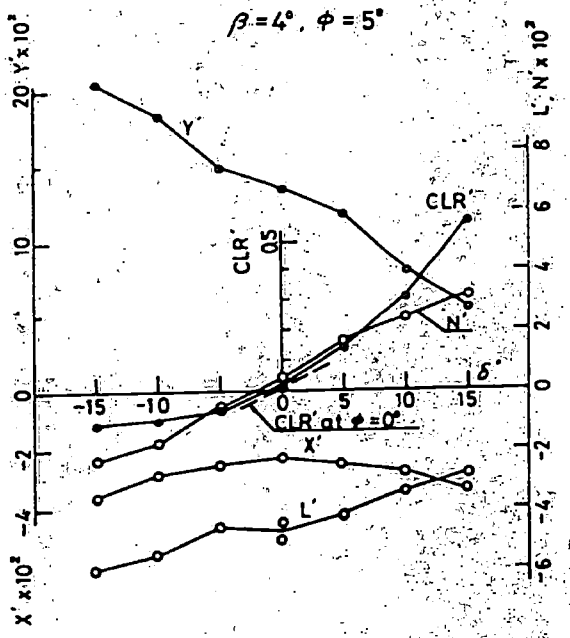

Fig. 19 Oblique Tow Test Result of Model C (3)

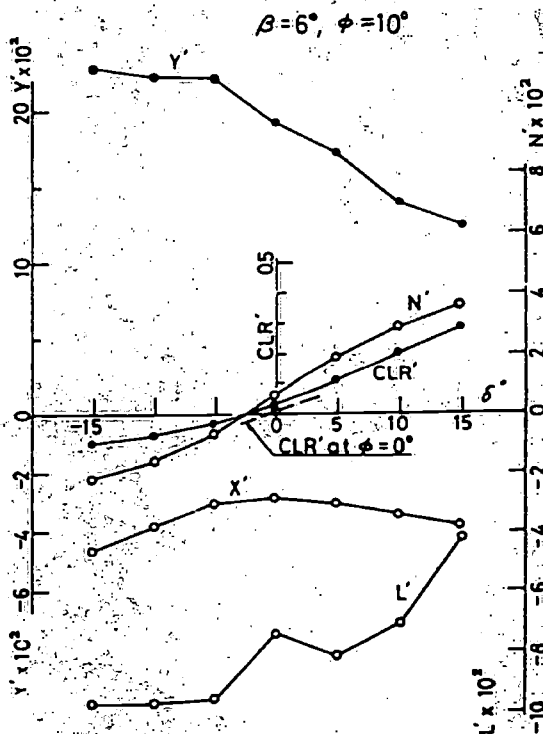

Fig. 20 Oblique Tow Test Result of Model C (4)

2.1 Geometric Theory ----- CLR, CE and Lead

This should perhaps be called a design practice rather than a theory, but is is the most popular procedure of getting a good balance of helm in design stage. CLR is defined as the centre of projected lateral area of the underwater part, hull, keel, skeg and rudder all included. In Fig.21 we indicate the "geometric CLR" thus defined, compared with the "hydrodynamic CLR" obtained by tank test.

At a glance we find the real centre of lateral resistance (hydrodynamic CLR) is considerably forward of the geometric CLR. The lead of hydrodynamic CLR over geometric CLR is 24% of L_{wl} for Model A, 14% for B and 9% for C.

Naval architects use C.E. and Lead together with the (geometric)CLR. C.E., Centre of Effort of Sails are defined as the centre of area of sails, all sheeted in amidship. Lead is the distance between CE and CLR, normally in percentage of L_{wl}. Most naval architects would choose the lead of about 20% for single-masted rig.

At any rate, the real centre of effort of sails is more or less apart from the geometric CE; the aerodynamic centre is not the geometric centre; easing a sheet in a reach run brings the real CE aftward. The geometric CLR is not the real CLR either. An empirical factor, "lead" is then called upon to compensate both errors. It should be noted, however, that the fore-and-aft balance of sails and underwater body does not only relate to helm balance under steady sailing. It does also have an essential effect on manoeuvring under sail, i.e.,luffing, tacking, paying-off and heaving-to. Being an empirical factor, the lead reflects consideration of these performances, not only of the balance of helm under steady sailing.

2.2 Slender Body Theory

The basic idea of this theory is "dynamic displacement effect" of a body moving through a liquid. Static displacement produces buoyancy. Dynamic displacement induces momentum change in the surrounding liquid, which generates a force acting upon the body.

A slender body means a body whose breadth and depth are much smaller than its length. We can compose the flow field around such a body by "laminating"two-dimensional lateral flow at each cross section plane. This is a great benifit for the analysis.

Now taking a slender-body moving through a liquid obliquely with a leeway angle, the hydrodynamics tells us that:

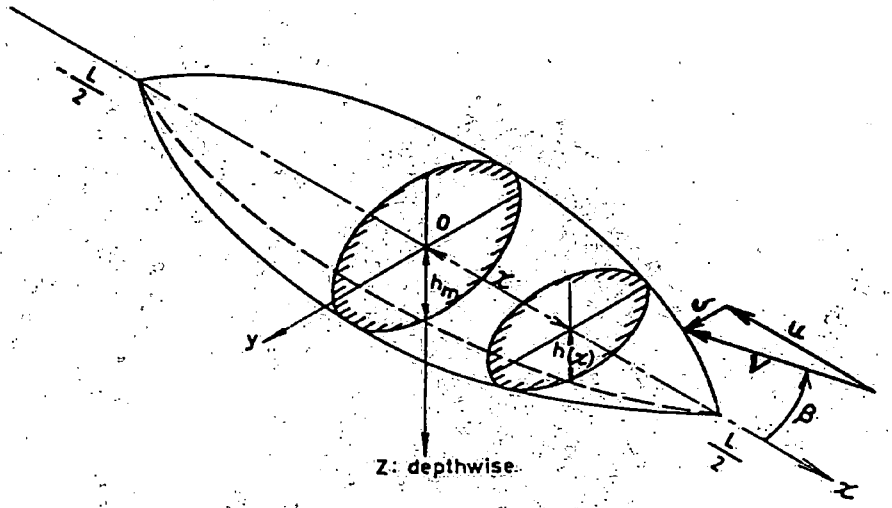

Fig.22 A Slender Body

Lateral momentum of the liquid in a plane perpendicular to the body's axis is $vA(x)$, where v is flow velocity normal to the body's axis and $A(x)$ is additional mass of the cross section of the body on the plane, x being measured along the axis. (cf. Fig.22).

Rate of change of lateral momentum in the plane is then

$$u\, v\, \frac{d}{dx} A(x) \tag{2}$$

where u is flow velocity along the body's axis.

The additional mass A is approximately

$$A(x) = \pi \rho\, h^2(x)$$

where $h(x)$ is half the local depth of the body as is shown in Fig.22.

The rate of change of momentum equals to local force acting on the cross section of the body. The resultant lateral force and its moment are:

$$Y = \pi\rho u \int_{-L/2}^{L/2} v \frac{d}{dx} h^2(x)\, dx \tag{3}$$

$$N = \pi\rho u \int_{-L/2}^{L/2} v\, x \frac{d}{dx} h^2(x)\, dx \tag{4}$$

This simply becomes :

$$Y = \pi\rho u^2\beta\int_{-L/2}^{L/2} dh^2 = \pi\rho u^2\beta\left[h^2(x)\right]_{-L/2}^{L/2} = 0 \qquad (5)$$

$$N = \pi\rho u^2\beta\left\{\left[x\cdot h^2(x)\right]_{-L/2}^{L/2} - \int_{-L/2}^{L/2} h^2(x)\,dx\right\}$$

$$= -\pi\rho u^2\beta\int_{-L/2}^{L/2} h^2(x)\,dx \qquad (6)$$

We get no lateral force (d'Alembert's paradox) but do get a moment even in an ideal fluid. This moment is often called Munk moment.

In the real fluid with viscosity, however, cross flow rounding the bottom of the body generates vortices trailing out from there. These vortices induce "wash down" flow which reduces the inflow angle to the afterbody. Accordingly on the afterbody, the lateral velocity v of Eqs. (3) and (4) becomes much smaller than leeway velocity $u\beta$. As the result the integral of Eq. (3) does not vanish, unlike Eq. (5), and we get some amount of lateral force. At the same time the moment N become smaller than of Eq. (6), Munk moment.

A popular assumption to deal with this effect is simply to cut off the integrations over the afterbody,[4] that is, to stop the integrations where $h(x)$ is maximum. This results in

$$Y = \pi\rho u^2\beta h_m^2 \qquad (7)$$

$$N = -\pi\rho u^2\beta\left\{x_m h_m^2 + \int_{x_m}^{L/2} h^2(x)\,dx\right\} \qquad (8)$$

where h_m : maximum half-depth of the body,
x_m : x where $h(x) = h_m$.

In applying this to sailing yachts we should halve the Y and N according to the principle of image on the waterplane.
The lateral resistance is simply

$$Y = \frac{\rho}{2}\pi v^2\beta d_m^2 \qquad (9)$$

where $V \cong u$ is ship speed in m/s., d_m the maximum draught, β angle of leeway in radian and ρ = 104 kg. $m^{-4}.sec^2$ for sea water.

The centre of lateral resistance is them

$$CLR = \frac{N}{Y} = x_m + \frac{1}{d_m^2} \int_{-L/2}^{L/2} h^2(x)\, dx \qquad (10)$$

where x_m : horizontal distance between the midship and the station where the draught is maximum ($h=d_m$), positive to forward of the midship.

$h(x)$: local draught, i.e., depth of the yacht below water line at station x.

The integration of Eq.(10) is performed by Simpson rule.

We applied this procedure to the Models A, B and C, Table 2 and Figs. 21 and 23 indicates the results. We have a fair result for the long-keel model A but at a small angle of leeway, say $\beta < 2°$ (cf.Fig.23). It is not surprising for the slender body lift theory is valid by its nature at an infinitesimal angle of attack. In larger leeway angle the covering effect of trailing vortices on the afterbody becomes less prominent. Consequently the rudder and stern deadwood produce an appreciable amount of lateral resistance: lateral resistance gradient Y'/β increases and CLR moves aftward. This is a remarkable feature of the long-keel model A, unlike the fin-keel Models B and C. The lifting surface theory of low aspect ratio is useful to take account of this effect. We will discuss it in Section 2.4. The lifting surface approach requires a fair amount of computation, however. So Eqs.(9) and (10) can perhaps be a practical procedure of evaluating the lateral resistance and CLR of long-keel boats with deep fore-foot (typical in Model A). We should remember in that case, however, that the lateral resistance gradient increases and CLR moves aftward both appreciably at larger leeway angle.

The whole underwater bodies of Models B and C including the fin-keel and rudder are not really slender;maximum draught is some 20% of L_{wl}. Nevertheless Table 2 show that this theory is not too bad to apply to these types of hulls. Errors in evaluating the lateral resistance are some 15%, and CLR error ranges 3 - 6% of L_{wl}, if we cut off the afterbody, including the rudder, at the maximum draught station.

To cut off entirely the contribution of the rudder to lateral resistance is perhaps an over simplification. A correction for this is to apply the same approach independently to the rudder to have rudder lateral force and then modify it by rudder force reduction factor. This reduction is assumed to come from the trailing vortices outflowing from the fin-keel. Table 2 and Fig.21 involves the results of such calculation

with rudder force reduction factor of 0.4.

2.3 Method of Gerritsma

This plain theory is recognized to give a good evaluation of the lateral resistance. To extend the fin-keel and rudder to the water surface and to take the image on the surface is a reasonable assumption from the hydrodynamics point of view. The bound vortex generated on the keel can not vanish at the bottom of the hull by the nature of vortex. Instead it induces a circulating flow around the hull about the vertical axis, and this effect is well represented by extending the bound vortex up to the surface.

The same reasoning can be applied to the rudder, though the trailing vortices coming out from the fin-keel reduces the inflow angle to the rudder considerably.[5] Table 2 and Fig.21 contain the lateral force and CLR calculated for Models B and C, following to this method. The reduction factor of 0.4 for the inflow angle to the rudder is based upon an analysis on the induced velocity (wash down) of the trailing vortices coming out from the keel.

This procedure without rudder force reduction gives a nice result in estimating the lateral resistance but the predicted CLR is rather too aft. The rudder force reduction improves the CLR prediction but the lateral resistance estimated is rather too small then.

2.4 A Combined Method of Vortex Wing and Slender Body Theory

The method of Gerritsma, based on the vortex wing theory, evaluates well the lateral resistance of the fin-keel and seperate rudder. That is certainly the essential part of lateral resistance of modern yacht hulls. What is lacking is, however, the contribution of the hull forebody, in the authors' view. Its share in lateral resistance may not be large, but it may have a considerable effect on yaw moment, and then on CLR.

This idea leads us to a combined method: to apply the vortex wing theory on the fin-keel and rudder (Gerritsma method) and the slender body lift theory on the forebody. The afterbody is exposed to the wash-down flow induced by the trailing vortices flowing out from the forebody and fin-keel. This eliminates the contribution of the afterbody to lateral resistance. (Jones assumption, cf. Section 2:2, reference 4). Strong wash down produced by the fin-keel will well justify this assumption.

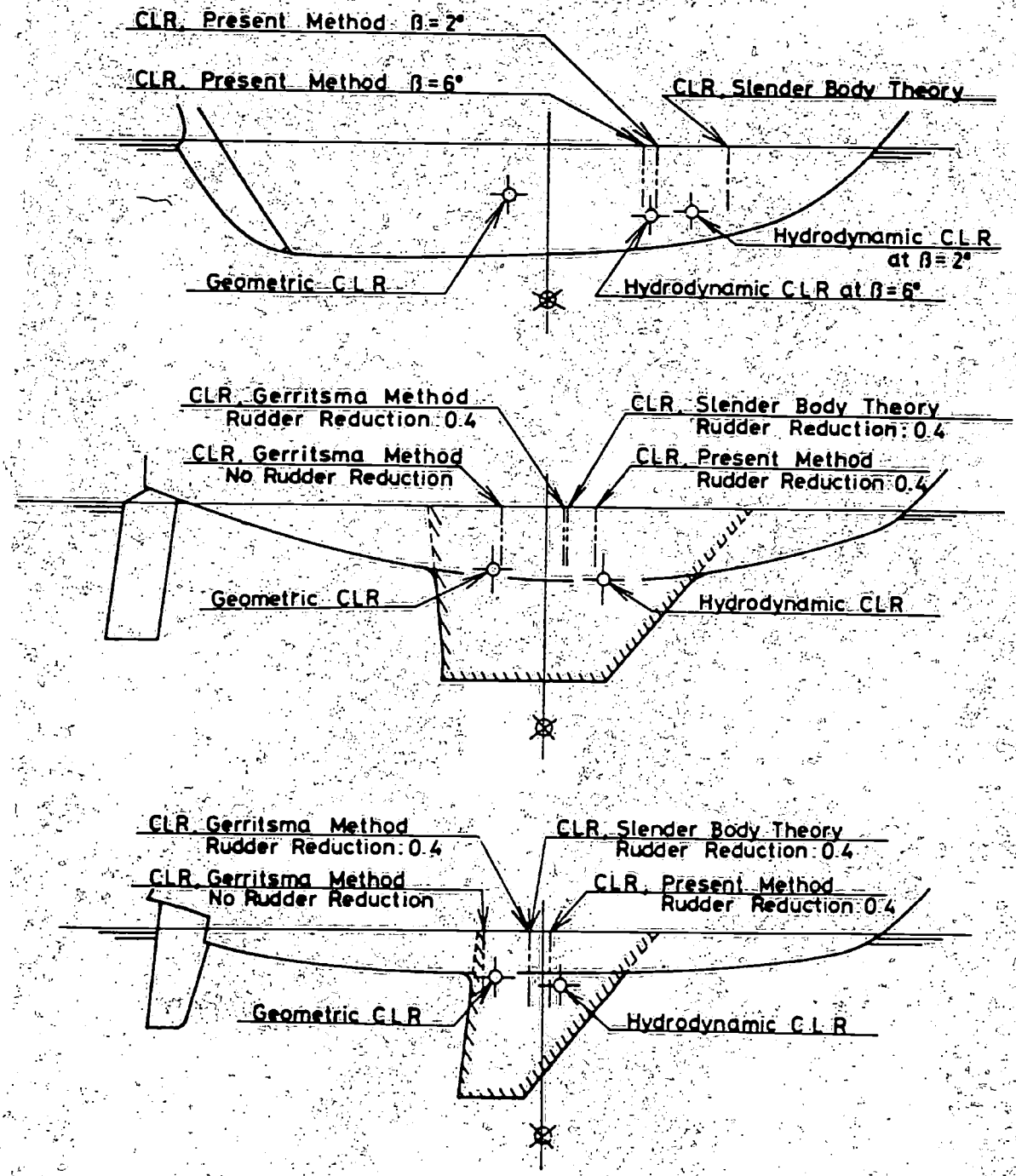

Fig.21 CLR Estimated through Various Procedures

Table 2 Lateral Resistance and CLR Estimated through Various Procedures

	Model A		Model B		Model C	
Procedures	Y'/β	CLR'	Y'/β	CLR'	Y'/β	CLR'
Tank Test	0.55, β=2° 0.77, β=6°	0.200, β=2° 0.146 β=6°	1.62	0.073	1.74	0.024
Geometric CLR		-0.078		-0.068		-0.067
Slender Body No Rudder Force	0.62	0.257	1.45	0.15	2.07	0.047
Slender Body Rudder Reduction:0.4			1.80	0.026	2.36	-0.018
Gerritsma No Rudder Reduction			1.70	-0.058	1.77	-0.082
Gerritsma Rudder Reduction:0.4			1.43	0.024	1.52	-0.018
Present Method No Rudder Reduction for Model A	0.527 β=2° 0.761 β=6°	0.155 β=2° 0.135 β=6°				
Rudder Reduction:0.4 for Models B and C			1.69	0.064	1.67	0.010

Y'/β and CLR' indicate average values over β =2°,4°,6° & 8° unless otherwise remarked.

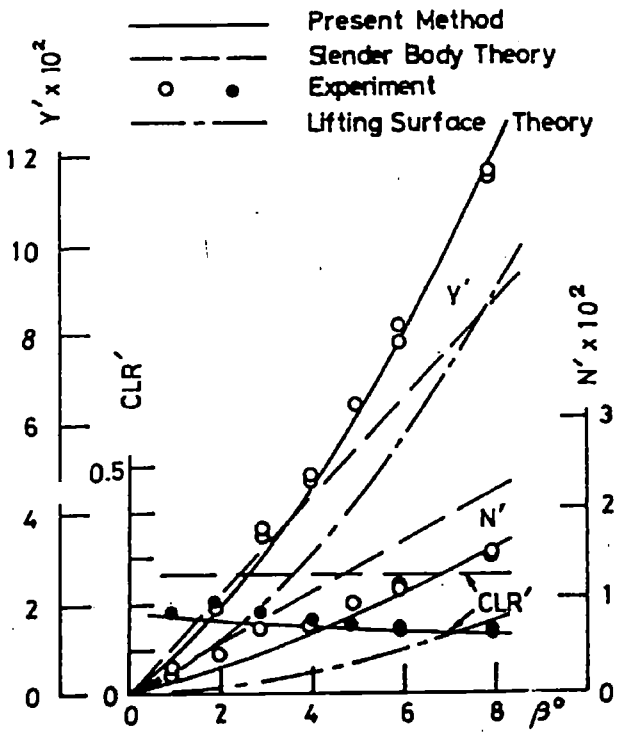

Fig. 23 Lateral Resistance and CLR Estimated through Various Procedure Compared with Tank Test Data of Model A.

The procedure is:

(1) to get the lateral resistance of the fin-keel and its moment about the midship, following to Gerritsma method, the lift gradient

$$p = \frac{\partial C_L}{\partial \alpha} = \frac{5.7\, a_e}{1.8 + \cos\Lambda \sqrt{\frac{a_e^2}{\cos^4\Lambda} + 4}} \qquad (11)$$

is used;

(2) to get the lateral resistance of the rudder and its moment similarly but with the rudder force reduction factor of 0.4;

(3) to use Eqs.(9) and (10) to obtain the lateral resistance of the fore-body and its moment about the midship, the draught h(x) in this case being that of the main hull (canoe-body);

(4) to sum up the above three to get the lateral resistance and CLR of the yacht.

The rudder reduction factor will vary configuration to configuration. 0.4 is perhaps a good average according to a hydrodynamic analysis on wash down flow behind a fin-keel.

Table 2 and Fig.21 tell us that this procedure works well for fin-keel models B and C. It will hopefully work also for a deep keel yacht with a shallow fore-foot and the rudder attached to the aft edge of the keel. In this case the rudder and deep keel should be regarded together as a single wing (like a fin-keel).

The long-keel, deep fore-foot Model A raises a problem: we can hardly define the keel to apply the vortex wing theory; the aspect-ratio of the equivalent wing must be very small any way, so that the lift gradient formula (11) may not be proper and the centre of pressure uncertain.

We tried a lifting surface approach instead of lifting line wing theory normally used in Gerritsma Method. The very low aspect-ratio of the long-keel Model A led us to the idea. The basic scheme is:

(1) to take a thin wing whose plan form is identical with the profile of the whole underwater body of Model A but including its image on the water-line;

(2) to distribute bound vortices continuously over the thin wing;

(3) to assume spanwise (depthwise) distribution of circulation uniform by the nature of very low aspect-ratio wing and consequently the same strength of free vortex trails out from the bottom of the keel;

(3) chordwise(lengthwise) distribution of circulation is assumed to be

$$\gamma_{(x)} \sqrt{\frac{1 + 2x/L}{1 - 2x/L}}$$

where $\gamma(x)$ is an unknown function of x, x being positive to forward;

(5) to get wash down velocity on the centre-line of the wing (i.e.water-line of the yacht) induced by all the bound and trailing vortices;

(6) to equate the wash down velocity with leeway lateral velocity $V\beta$ to have an integral equation to define $\gamma(x)$;

(7) to approximate $\gamma(x)$ by a trigonometric series with a number of unknown constants and put it into the integral equation to deliver a set of simultaneous equations to define the unknown constants.

(8) to get the resultant lateral force and its moment by summing up all the bound vortex circulations thus defined.

The lateral force and its moment obtained in this manner for Model A is indicated by chain lines in Fig.23. The upward curvature of lateral force curve is clearly seen.

To add the lateral force and moment of the canoe-body upon the ones obtained through this lifting surface approach can be controversial. We tried this, however, and the result looks good indeed at least in this case. A possible interpretation is that the lifting surface approach evaluates the lift of the skelton thin wing and the slender body theory the dynamic displacement lift of the main hull (canoe body). The lateral force and moment of the canoe-body is given by Eqs.(9) and (10) also in this case.

3. PERFORMANCE PREDICTION AND ELEMENTS OF BALANCE OF HELM

3.1 Performance Prediction

Let us assume a jib-headed sloop rig for all the three Models A, B and C. The length over all of actual vessels is assumed to be 10 metres. Sail area is $56m^2$ and the mast height above the surface 13 metres (cf. Fig.24) The aerodynamic data of this rig is provided by model sail test[2] as is illstrated in Fig.24 in a non-dimensional form. The notations employed are:

$X'_s = X_s / \frac{1}{2} \rho_a S U^2$ $\quad X_s$: longitudinal (thrust) component of sail force

$Y'_s = Y_s / \frac{1}{2} \rho_a S U^2$ $\quad Y_s$: lateral component of sail force

$N'_S = N_S / \frac{1}{2} \rho_a S^{3/2} U^2$ N_S : yaw moment of sail force about the mast

ρ_a : density of air in $kg.m^{-4}.sec^2$ S : sail area in m^2

U : apparent wind speed in m/sec.

Now we can make a sailing performance prediction of the yachts A,B and C by incorporating the sail data with the tank test data of section 1. The fundamental equations are :

$$X' (V, \beta, \delta, \phi) \frac{\rho_A}{\rho_a S} (\frac{V}{U})^2 = X'_S (\gamma_A, \phi) \quad (12)$$

$$Y' (\beta, \delta, \phi) \frac{\rho_A}{\rho_a S} (\frac{V}{U})^2 = Y'_S (\gamma_A, \phi) \quad (13)$$

$$N' (\beta, \delta, \phi) \frac{\rho_A L_{WL}}{\rho_a S^{3/2}} (\frac{V}{U})^2 = N'_{SO} (\gamma_A, \phi) \quad (14)$$

$$W \; GZ(\phi) = \frac{\rho_a}{2} S^{3/2} U^2 L'_S (\gamma_A, \phi) \quad (15)$$

where γ_A : apparent wind direction. N_{SO} : yaw moment of sail force about the midship (converted from N_S)

The sail trim is adjusted so as to produce the maximum thrust (X force) for a given γ_A.

Given apparent wind condition i.e., U and γ_A, we obtain heel ϕ, leeway β, speed V and rudder angle δ from the four equations, (12),(13) (14) and (15). Then we get the true wind speed U_T and its direction γ_T by vector calculation. By interpolation finally we get V, β, δ and ϕ for a given U_T and γ_T.

Figs. 25 and 26 illustrate the result. The true wind speed is 8m/s. Superior speed of the light displacement IOR racer is impressive. At the same time the 19th century redningskoite competes well with the medium displacement cruiser of the present day, though her windward ability is the worst among the three.

3.2 Elements of Balance of Helm

Fig.26 illustrates the rudder angle versus apparent wind direction, as obtained by the performance prediction. These rudder angles are called upon to balance the helm at different point of steady sailing. Sorting out the calculation of the performance prediction stage by stage tells us that the rudder angle at steady sailing are composed of three components:

(1) the first is a rudder angle required to counteract a couple generated by sail and hull lateral forces, i.e. δ_1 due to unbalance of aerodynamic CE and hydrodynamic CLR;

(2) the second is to counteract a yaw moment acting on a heeled hull, i.e. δ_2 due to shift of hydrodynamic CLR induced by heel;

(3) the last is to counteract a yaw moment generated by leeward shift of sail driving force accompanied with heel, δ_3.

The last yaw moment is evaluated approximately by

$$X_s \frac{h}{2} \sin \phi = X \frac{h}{2} \sin \phi$$

where X_s and X are sail thrust and hull resistance respectively, and h is the mast height above the surface; $\frac{h}{2}$ is then approximately the CE height above the water.

As is seen in Fig.26 the last element of rudder angle is the largest in most cases. In other words the common trend of weather-helm accompanied with steep heel is primarily due to the leeward shift of driving force of sails. The forward shift of centre of lateral resistance induced by heel certainly has some effect but it is rather small, perhaps somewhat contrary to the common belief among sailors.

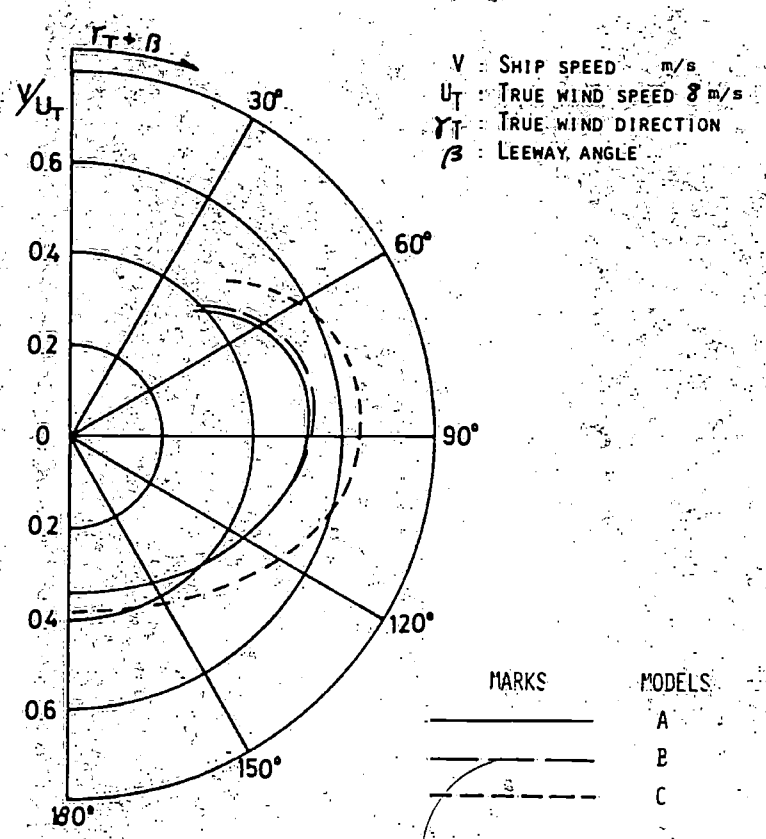

Fig.25 Speed Polar Diagram Obtained by Performance Prediction

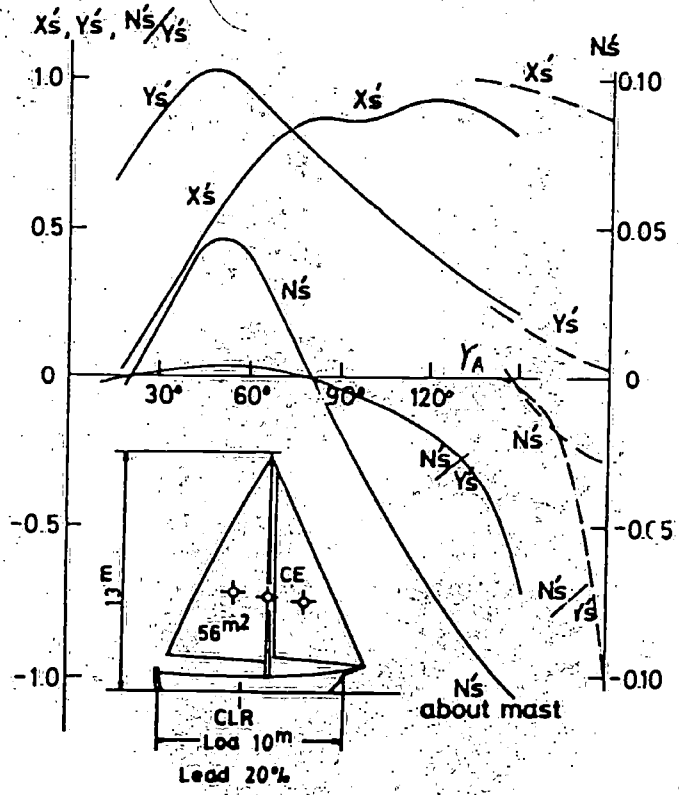

Fig.24 Sail Data for Performance Prediction[2)]

δ_1 : due to unbalance of CE and CLR

δ_2 : due to shift of CLR induced by heel

δ_3 : due to leeward shift of drive force of sails induced by heel

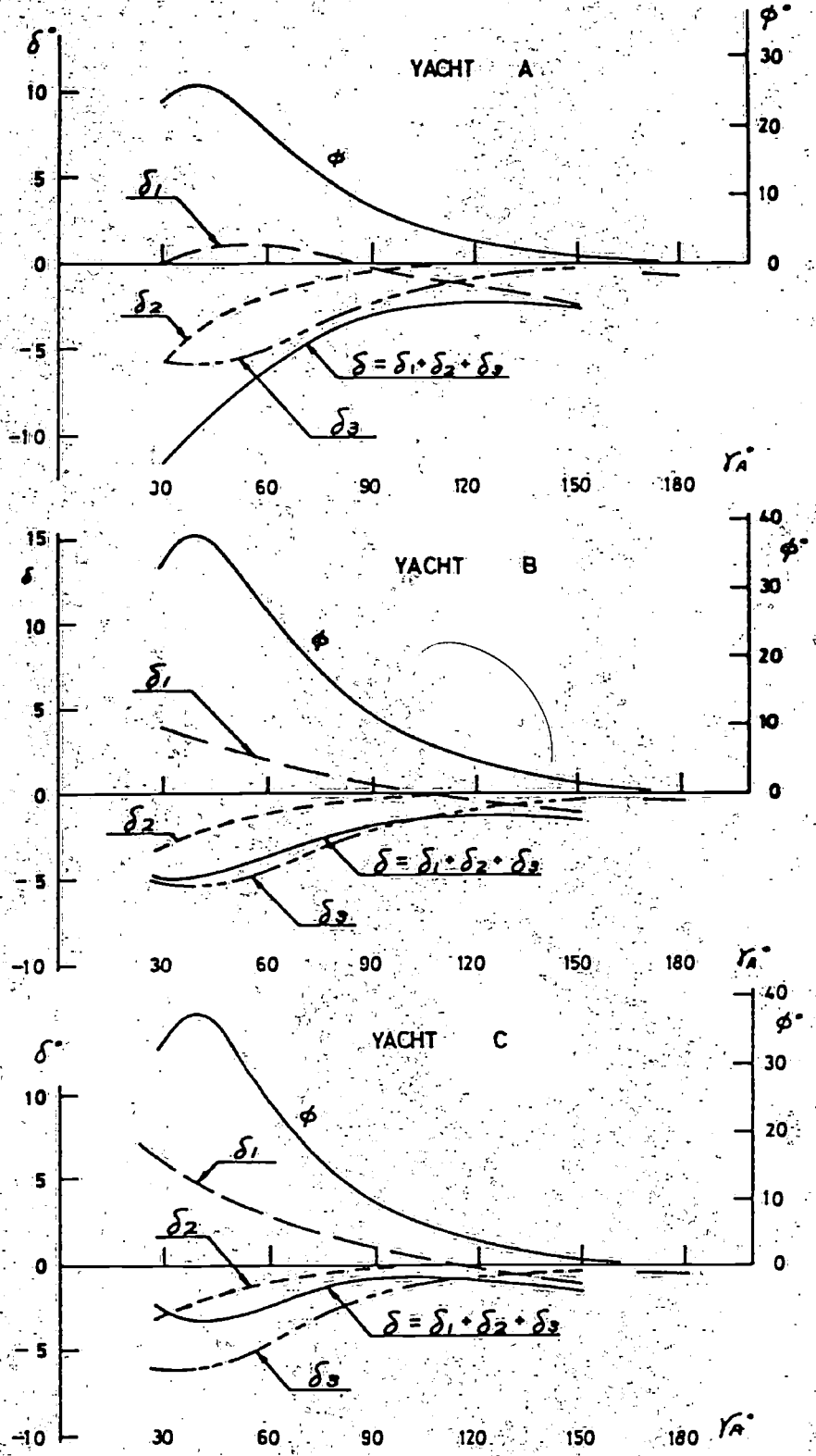

Fig. 26 Rudder Angle Needed for Helm Balance at Steady Sailing and Its Components.

References

1. Letcher Jr., J. S. : Balance of Helm and Static Directional Stability of Yachts Sailing Close-Hauld, Jounal of the Royal Aieronautical Society, Vol. 69, April 1965.
2. Nomoto, K., Tatano, H., Kaneda, T. : Hydrodynamic Analysis on Sailing (lst Report), Journal of the Kansai Society of Naval Architects, Japan, No. i70, September 1978.
3. Gerritsma, J. : Course keeping qualities and motions in waves of a sailing yacht, Proceedings of the third AIAA Symposium on Aero-hydrodynamics of Sailing, California, 1971.
4. Jones, R. T. : Properties of Low Aspect Ratio Pointed Wings at Speeds above and below the Speed of Sound, NACA Tech. Report, 835, 1961.
5. Beukelman, W. and Keuning, J. A. : The Influence of Fin Keel Sweep-Back on the Performance of Sailing Yachts, 4th HISWA Symposium on Yachtarchitecture, 1975.